

Noninvasive Imaging of Dendrimer-Type N-Glycan Clusters: In Vivo Dynamics Dependence on Oligosaccharide Structure**

Katsunori Tanaka,* Eric R. O. Siwu, Kaori Minami, Koki Hasegawa, Satoshi Nozaki, Yousuke Kanayama, Koichi Koyama, Weihsu C. Chen, James C. Paulson, Yasuyoshi Watanabe, and Koichi Fukase*

Among the various types of oligosaccharide structures, asparagine-linked oligosaccharides (N-glycans) are the most prominent in terms of diversity and complexity. In particular, N-glycans containing sialic acid residues are involved in a variety of important physiological events, including cell–cell recognition, adhesion, signal transduction, and quality control.^[1] Moreover, it has long been known that the sialic acids in N-glycans on soluble proteins or peptides enhance circulatory residence,^[2] that is, N-glycan-engineered erythropoietin (EPO)^[2b] and insulin^[2c] exhibit a remarkably higher stability in serum, which effects their prolonged bioactivity. Antibody-dependent cellular cytotoxicity (ADCC) and/or complement-dependent cytotoxicity (CDC) have also been proposed to be modulated by the sialic acids of N-glycans in immunoglobulin G (IgG) through Siglec interactions by glycosylating or removing the sialic acids.^[3] However, these

important findings and previous efforts in investigating N-glycan functions have been mostly based on in vitro experiments using isolated lectins, cultured cells, and dissected tissues. Recently, interest has shifted to the dynamics of these glycans in vivo, that is, how the function and/or interaction of the individual N-glycan works synergistically through dynamic processes in the body to eventually exhibit biological phenomena. Molecular imaging^[4–6] is the most promising tool to visualize the “on-time” N-glycan dynamics in vivo.

The challenge in efficient glycan imaging in living animals is to obtain the structurally pure oligosaccharides from nature or by synthetic methods.^[7] In addition, the bioactivity of the oligosaccharides might be derived from the multivalency and/or heterogeneous environment, that is, on cell surfaces that are composed of oligosaccharide clusters along with other biomolecules.^[1] A single molecule of the N-glycan, obtained from either a natural or synthetic source, is readily excreted from the body.^[8] Thus, efficiently mimicking and labeling such an N-glycan-involved bioenvironment, for example, by conjugating the N-glycans to the liposomes, to the clusters, or even to the surface of the cells,^[9] may provide information on the “in vivo dynamics” of N-glycans. The recent successful noninvasive imaging and biodistribution study of glycans and glycoconjugates dealt with natural^[10] and neo-glycoproteins, liposomes, and nanoparticles.^[11]

Herein, we report the first fluorescence and positron emission tomography (PET) imaging of dendrimer-type glycoclusters using the multivalency effects of 16 molecules of N-glycans. A variety of N-glycan clusters were efficiently prepared based on the Cu^I-mediated “self-activating” Huisgen 1,3-dipolar cycloaddition,^[12] and the remarkable dependence of the in vivo dynamics on the structure of sialic acids and organ-specific accumulation were discovered for the first time.

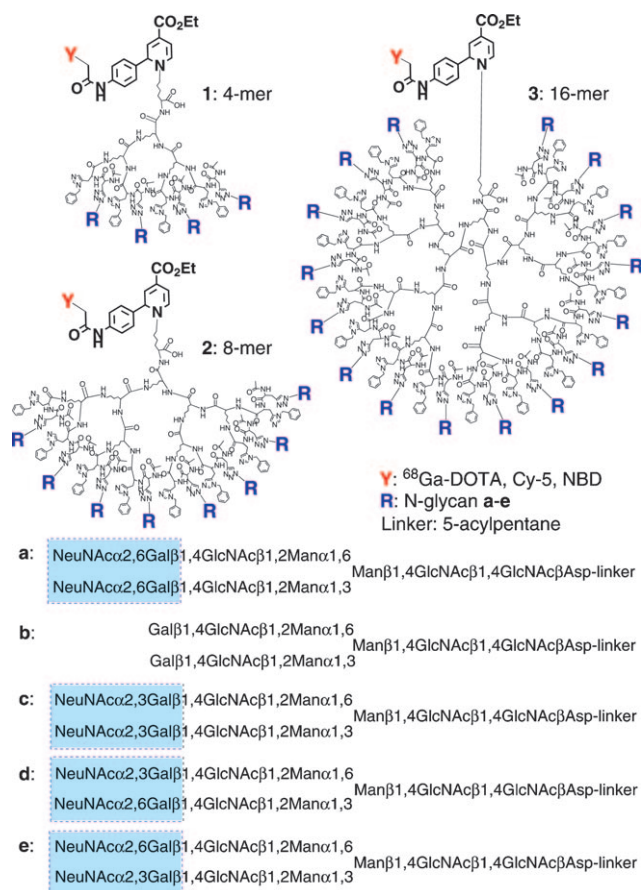
We designed polylysine-based dendrimer-type glycoclusters (Scheme 1); the different generations of clusters, namely those consisting of four (4-mer **1**), eight (8-mer **2**), and 16 (16-mer **3**) molecules of N-glycan derivatives (**a–e**),^[13] were investigated to examine cluster (multivalency) effects^[1,14] on in vivo dynamics. The clusters were designed to have a terminal lysine ϵ -amino group so that they could be efficiently labeled by fluorescent groups or ⁶⁸Ga-1,4,7,10-tetraazacyclododecane-1,4,7,10-tetraacetic acid (⁶⁸Ga-DOTA) as the PET radiolabel in the presence of numerous hydroxy groups through our 6 π -azaelectrocyclization protocol under mild conditions.^[10] The polylysine-based dendrimer core with terminal histidine and propargyl glycine residues could be

[*] Dr. K. Tanaka,^[†] Dr. E. R. O. Siwu,^[†] K. Minami, Prof. Dr. K. Fukase
Department of Chemistry
Graduate School of Science, Osaka University
1-1 Machikaneyama-cho, Toyonaka-shi, Osaka 560-0043 (Japan)
Fax: (+81) 6-6850-5419
E-mail: ktzenori@chem.sci.osaka-u.ac.jp
koichi@chem.sci.osaka-u.ac.jp
Homepage: <http://www.chem.sci.osaka-u.ac.jp/lab/fukase/>
Dr. K. Hasegawa, Dr. S. Nozaki, Dr. Y. Kanayama,
Prof. Dr. Y. Watanabe
RIKEN Center for Molecular Imaging Science
6-7-3 Minatojima, Chuo-ku, Kobe-shi, Hyogo 650-0047 (Japan)
K. Koyama
Kishida Chemical Co., Ltd.
14-10 Technopark, Sanda-shi, Hyogo 669-1339 (Japan)
Dr. W. C. Chen, Prof. J. C. Paulson
Department of Chemical Physiology, Joint Department of Molecular
Biology, The Scripps Research Institute
10550 North Torrey Pines Road, MEM-L71, La Jolla, CA 92037 (USA)

[†] These authors contributed equally to this work.

[**] We thank Kazuhiro Fukae, Azusa Hashimoto, and Jun Igarishi, Otsuka Chemical Co., Ltd., for supplying N-glycans. This work was supported in part by Grants-in-Aid for Scientific Research Nos. 19681024 and 19651095 from the Japan Society for the Promotion of Science, Collaborative Development of Innovative Seeds from the Japan Science and Technology Agency (JST), New Energy and Industrial Technology Development Organization (NEDO, project ID: 07A01014a), research grants from Yamada Science Foundation as well as the Molecular Imaging Research Program, and Grants-in-Aid for Scientific Research from the Ministry of Education, Culture, Sports, Science, and Technology (MEXT) of Japan.

Supporting information for this article is available on the WWW under <http://dx.doi.org/10.1002/anie.201000892>.



Scheme 1. Generation and structures of glycoclusters. NBD = nitrobenzoxadiazole.

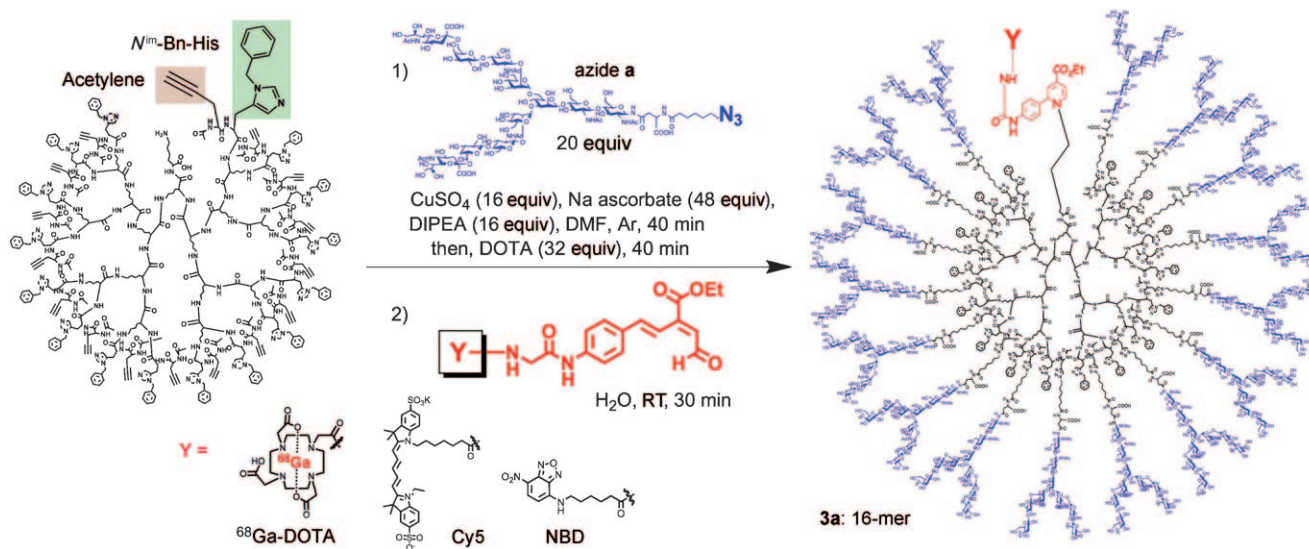
synthesized by a solid-supported protocol (see the Supporting Information).

N-Glycans were subsequently introduced by “self-activating” Huisgen 1,3-dipolar cycloaddition^[12] (reaction between

acetylene on the polylysine template and azide on the N-glycans, Scheme 2). Examples include the terminal acetylene of the polylysine-based dendrimer (Scheme 2), which was smoothly reacted with azide partner **a**, bis- α Neu(2–6)Gal containing complex-type N-glycan (see the Supporting Information for preparation of azide derivatives) in the presence of equimolar amounts of copper sulfate and sodium ascorbate, and diisopropylethylamine (DIPEA; each relative to the N-glycan molecules) at room temperature for 40 min (see HPLC monitoring of the reaction in the Supporting Information). The residual copper ions were removed by chelation with DOTA and size-partitioning centrifugal filtration. Subsequent HPLC purification gave tetra-glycocluster **1a** (4-mer), octa-glycocluster **2a** (8-mer), and hexadeca-glycoclusters **3a–e** (16-mers) with a molecular weight of circa 50 kDa in almost quantitative yields (see Schemes 1 and 2).

Detection of the mother ions by MALDI-TOF analyses,^[15] HPLC patterns of size-partitioning gel filtration, and the integration of the representative sugars, triazole, His, and Lys signals in their ^1H NMR spectra all confirmed the desired clusters (see the Supporting Information). These clusters were subsequently labeled by DOTA or NBD and Cy5 fluorophores through rapid 6π -azaelectrocyclization (see Scheme 2 and the Supporting Information).^[9,10] The incorporation of ^{68}Ga in DOTA-labeled glycoclusters **1a–3e** was performed by slightly modifying the procedures previously described^[16] by reaction with ^{68}Ga in 4-(2-hydroxyethyl)-1-piperazineethanesulfonic acid (HEPES) buffer (pH 3.5, 95 °C, 15 min) and subsequent HPLC purification (see the Supporting Information).

Throughout the following imaging studies by both PET and fluorescence detection, glycoclusters **1a–3e** (500 pmol) labeled with ^{68}Ga -DOTA and Cy5 (excitation at 646 nm, emission at 663 nm) were administered to the tail vein of BALB/c nude mice ($n = 3$) prior to whole-body scanning over 4 h. We initially examined the PET of glycoclusters **1–3**, which consisted of bis-Neu α (2–6)Gal-containing glycan (**a**), asialo-



Scheme 2. Preparation of N-glycan clusters through histidine-accelerated Cu^{I} -mediated Huisgen 1,3-dipolar cycloaddition and labeling by 6π -azaelectrocyclization. Bn = benzyl.

glycan (**b**), and bis-Neu α (2-3)Gal-glycan (**c**). Prior to injection, the radioactivity of each ^{68}Ga -DOTA-labeled glycocluster was adjusted to 10 MBq.

First, the *in vivo* dynamics between the generations of clusters, namely those between the 4-mer (**1a**), 8-mer (**2a**), and 16-mer (**3a**), differed remarkably (Figure 1a–c).

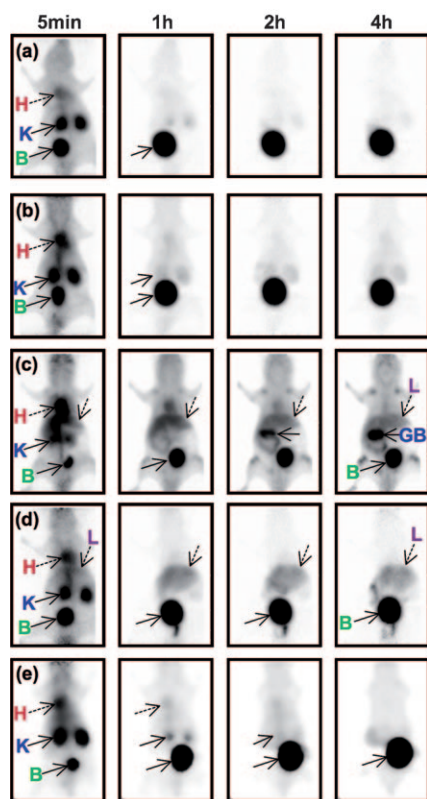


Figure 1. Dynamic PET imaging of glycoclusters **1a**, **2a**, and **3a–c** (a–e, respectively) in normal BALB/c nude mice. ^{68}Ga -DOTA-labeled glycoclusters (10 MBq) were administered into the tail vein of the mice ($n = 3$, 500 pmol, 100 μL /mouse) and the whole body was scanned by a small-animal PET scanner, microPET Focus 220 (Siemens Medical Solutions Inc., Knoxville, TN, USA), over 0–4 h after injection; H: heart; K: kidney; L: liver; B: urinary bladder; GB: gallbladder.

Although 4-mer **1a** and 8-mer **2a** were rapidly and almost completely cleared through the kidney (then to the urinary bladder) over 1 h (Figure 1a and b), the radioactivity derived from 16-mer **3a** was still retained in the body after 4 h (Figure 1c), but was excreted slowly from the kidney/urinary bladder and from the gallbladder (intestinal excretion pathway). A biodistribution study of the dissected tissues after 4 h detected the ^{68}Ga radioactivity of **3a** mostly in the liver, gallbladder, and blood, then in the order of the lungs, kidney, colon, pancreas, and spleen (see the Supporting Information). These results clearly show the significant cluster and/or multivalency effects on the *in vivo* dynamics. Hence, the 16-mer cluster should be well suited for further biodistribution analyses by N-glycan imaging, but the 32-mer glycocluster would be unsuitable for *in vivo* dynamics studies because of its high molecular weight (ca. 100 000), and thus was not considered for these experiments.

The differences in the clearance properties between the 4-mer, 8-mer, and 16-mer may be a result of their molecular size,^[17] that is, the smaller 4-mer and 8-mer can be easily cleared through biofiltration in the kidney. In fact, the glomerular capillary wall in the kidney is highly permeable to water, electrolytes, and substances with relatively small molecular weights, while larger molecules such as myoglobin are filtered to a lesser degree.^[17]

Alternatively, the degree of negative charge (the number of sialic acid residues) and/or degree of hydrophilicity of the clusters, that is, hydrophilic N-glycans versus the hydrophobic polylysine backbone occupying the surface of the clusters, may affect rapid clearance through the kidney. For example, the 4-mer and 8-mer, which have a more hydrophobic nature, may be trapped by scavenger receptors in the serum, similar to the degradation process for the “misfolded” hydrophobic glycoproteins inside the endoplasmic reticulum (ER; quality control of glycoproteins).^[18]

We subsequently examined the *in vivo* dynamics and biodistribution of asialo-glycan **3b** and bis-Neu α (2-3)Gal glycan **3c** using the 16-mer polylysine template (Scheme 1). Unlike the case of bis-Neu α (2-6)Gal **3a** (Figure 1c), the asialo-glycan cluster **3b** rapidly cleared through the kidney to the bladder (Figure 1d), although some accumulation was observed in the liver because the asialoglycoprotein receptors are highly expressed in this organ.^[2a] Dissection experiments after 4 h also found the strongest accumulation in the liver followed by the gallbladder and slight accumulation in the colon and kidney (see the Supporting Information). The results are consistent with our recent PET analyses of glycoproteins, orosomucoid, and asialoorosomucoid,^[10] where the asialo congener is more rapidly excreted than orosomucoid through the kidney as well as the liver/gallbladder pathways (leading to intestinal excretion). However, the α linkage to the 3-OH of galactose in glycocluster **3c**, which also contains sialic acid, was readily excreted through the kidney/urinary bladder as shown in Figure 1e.^[19] These PET results on the 16-mer glycoclusters **3a–c** suggest that the specific sialoside linkage to galactose, that is, the Neu α (2-6)Gal linkage, in N-glycan structures plays an important role in the circulatory residence of N-glycans, which in turn results in uptake of **3a** in the liver (see Figure 1c and the Supporting Information). In addition, this specific sialoside linkage markedly differentiates the excretion mechanism from those of the asialo and Neu α (2-3)Gal cases, which proceed through a biofiltration pathway in the kidney.

The prolonged *in vivo* lifetime of the sialic acid-containing glycoclusters agrees with the well-known hypothesis of the clearance of the asialoglycoproteins through the asialoglycoprotein receptors.^[2a,20] However, the notable difference in the serum stability as a result of the sialoside bond linkages to the galactose, that is, the α (2-6) versus α (2-3) linkages, is an intriguing observation.^[19] These dynamic PET images suggest a new receptor-mediated excretion mechanism for Neu α (2-3)Gal-containing glycans, which usually cannot be found in serum. Alternatively, the “excretion-escaping” mechanism, by stimulating the immunosuppressive signals through the immunoreceptor tyrosine-based inhibitory motif (ITIM) molecules through Siglec families,^[21] may account for the

higher stability of Neu α (2-6)Gal-glycan (see below). The combination of high valency and long circulatory half-life (reduced clearance) of Neu α (2-6)Gal-glycan most likely leads to the uptake of **3a** by hepatocytes through the Gal/GalNAc lectin receptor.^[22,23] The “polar transport mechanism”,^[24] which “tags” the fucose to specific N-glycans in the liver, could also explain the slow clearance of bis-Neu α (2-6)Gal cluster **3a** through the gallbladder.

In light of the strikingly different in vivo dynamics and excretion pathways between the N-glycan clusters **3a–c**, a biodistribution study of the glycoclusters **3a–e** was performed in more detail by using fluorescence imaging (Figure 2).

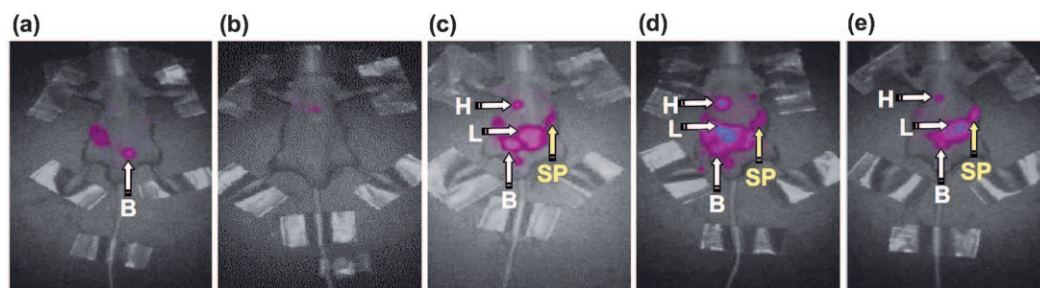


Figure 2. a–e) Dynamic fluorescence imaging of glycoclusters **3a–e** in BALB/c nude mice: a) **3b**; b) **3c**; c) **3a**; d) **3d**; e) **3e**. Cy5-labeled glycoclusters **3a–e** were administered into the tail vein of the mice ($n=3$, 500 pmol, 100 μ L/mouse) and whole-body scans were performed from the front side by eXplore Optix, GE Healthcare (excitation 646 nm, emission 663 nm) 4 h after injection. Data were normalized. H: heart; L: liver; B: urinary bladder; SP: spleen.

Clusters **3d** and **3e**, which contain mixed Neu α (2-6)Gal and Neu α (2-3)Gal moieties, were particularly interesting because the circulatory stability was notably enhanced by Neu α (2-6)Gal, but not by Neu α (2-3)Gal, disaccharides. Thus, as visualized by fluorescence imaging (Figure 2), glycoclusters **3a**, **3d**, and **3e**, which contain at least one Neu α (2-6)Gal nonreducing end motif, showed higher stabilities in vivo than asialo and Neu α (2-3)Gal congeners **3b** and **3c**. The Cy5 fluorescence derived from clusters **3a**, **3d**, and **3e** was eventually accumulated mostly in the liver, presumably because of the interaction with asialoglycoprotein receptor,^[22] but was also observed in the spleen after 4 h (Figure 2c–e). Out of the three glycoclusters, **3e**, which contains both Neu α (2-6)Gal and Neu α (2-3)Gal nonreducing end structures (from the 6- and 3-hydroxy groups of branching mannose, respectively), showed the highest fluorescence intensity in the spleen (Figure 2e).

The spleen is an organ located in the abdomen, and it functions in the destruction of old, aged red blood cells as well as holding a reservoir of blood. Moreover, it can function as part of the immune system, such as the reticuloendothelial system (RES), or in the production of antigen-specific antibodies by interacting T cells with mature B cells. Because Siglec 2 (CD22),^[21,25] which is a Neu α (2-6)Gal-specific lectin, is overexpressed in mature B cells and is responsible for immune-negative regulations, we examined the possibility of an interaction with our clusters **3a–e** (see the Supporting Information). The A20 B-cell line (expressed murine CD22), and Daudi B-cell line (expressed human CD22)^[26] only

detected a weak interaction with these clusters; cluster **3d** exhibited the weakest interaction. Therefore, Neu α (2-6)Gal-containing clusters **3a**, **3d**, and **3e** are most likely captured by the RES, which consists of phagocytic cells such as monocytes and macrophages that traffic to the spleen and liver as the reticular connective tissues. Yet during capture by the RES, stimulation by an “immune-suppressive signal”, through Neu α (2-6)Gal–Siglec interactions on the phagocytic cells,^[21] cannot be ruled out to explain the serum stability of these clusters. Overall, these in vivo images clearly visualize the importance of at least one Neu α (2-6)Gal moiety in the circulatory residence of the N-glycans and the precise

regulation of the bio-distribution by a combination of the α (2-6)- and α (2-3)-sialoside linkages.

Additionally, an examination of glycoclusters **3a–e** in a cancer model was performed (see the Supporting Information). Although these clusters did not target the tumor tissue (DLD-1 implanted to the left femoral regions), markedly different in vivo dynamics were

observed from those in normal mice. For example, excretion rates of glycoclusters **3d** and **3e** were accelerated in the cancer-affected mice and accumulation was not detected in the spleen, whereas the excretion rate of **3b** was considerably suppressed in the cancer mice (see the Supporting Information). Although the phenomena could not be explained by the currently available data, these differences make N-glycan clusters applicable to a new class of diagnostic probes.

This study has, for the first time, demonstrated a marked difference in the in vivo dynamics and biodistributions between α (2-6) and α (2-3)sialosides, through a multivalent effect proven to allow high selectivity and affinity in ligand–protein interactions.^[14,27] Totally different dynamics of the N-glycans between the normal and tumor models were also discovered by the present investigation. These results indicate the importance and validity of in vivo molecular imaging in living animals. Research directed towards targeting cancer, inflammation, and immune-related organs by using the developed glycoclusters is currently under way.

Experimental Section

General preparation procedure of glycoclusters (preparation of **3a):** CuSO₄ (64 μ g, 3.2×10^{-4} mmol), sodium L-ascorbate (238 μ g, 1.2×10^{-3} mmol), and DIPEA (74 nL) were added to a solution of acetylene-containing polylysine (16-mer, 158 μ g, 2.0×10^{-5} mmol) and azide **a** (1.0 mg, 4.0×10^{-4} mmol) in DMF (50 μ L) and H₂O (50 μ L) at room temperature. After the mixture had been stirred for 40 min at this temperature, DOTA (647 μ g, 1.56×10^{-3} mmol) was added and the resulting solution was stirred for another 40 min. Low-

molecular-weight compounds were removed by filtration using a Microcon centrifugal filter (YM-10, 10000 cut, Millipore), and the resulting aqueous solution was lyophilized to give glycocluster **3a** as an amorphous solid (960 µg, quant.). Reverse-phase HPLC, size-partitioning gel filtration analysis, ¹H NMR spectroscopy, and MALDI-TOF mass spectrometry data are shown in the Supporting Information.

Received: February 12, 2010

Revised: July 16, 2010

Published online: September 20, 2010

Keywords: antitumor agents · dendrimers · fluorescent probes · oligosaccharides · positron emission tomography

- [1] *Analysis of Glycans, Polysaccharide Functional Properties & Biochemistry of Glycoconjugate Glycans, Carbohydrate-Mediated Interactions: Comprehensive Glycoscience: From Chemistry to Systems Biology, Vols. II & III* (Eds.: J. P. Kamerling, G.-J. Boons, Y. C. Lee, A. Suzuki, N. Taniguchi, A. G. J. Voragen), Elsevier, **2007**.
- [2] a) A. G. Morell, R. A. Irvine, I. Sternlieb, I. H. Scheinberg, G. Ashwell, *J. Biol. Chem.* **1968**, *243*, 155–159; b) S. Elliott, T. Lorenzini, S. Asher, K. Aoki, D. Brankow, L. Buck, L. Busse, D. Chang, J. Fuller, J. Grant, N. Hernday, M. Hokum, S. Hu, A. Knudten, N. Levin, R. Komorowski, F. Martin, R. Navarro, T. Osslund, G. Rogers, N. Rogers, G. Trail, J. Egrie, *Nat. Biotechnol.* **2003**, *21*, 414–421; c) M. Sato, T. Furuike, R. Sadamoto, N. Fujitani, T. Nakahara, K. Niikura, K. Monde, H. Kondo, S. I. Nishimura, *J. Am. Chem. Soc.* **2004**, *126*, 14013–14022.
- [3] Y. Kaneko, F. Nimmerjahn, J. V. Ravetch, *Science* **2006**, *313*, 670–673.
- [4] a) M. Suzuki, R. Noyori, B. Langstom, Y. Watanabe, *Bull. Chem. Soc. Jpn.* **2000**, *73*, 1053–1070; b) T. Hosoya, K. Sumi, H. Doi, M. Wakao, M. Suzuki, *Org. Biomol. Chem.* **2006**, *4*, 410–415.
- [5] a) K. Tanaka, K. Fukase, *Org. Biomol. Chem.* **2008**, *6*, 815–828; b) K. Tanaka, K. Fukase, *Mini-Rev. Org. Chem.* **2008**, *5*, 153–162.
- [6] a) T. Ido, C. N. Wan, V. Cassela, J. S. Fowler, A. P. Wolf, *J. Labelled Compd. Radiopharm.* **1978**, *14*, 175–183; b) S. S. Gambhir, *Nat. Rev. Cancer* **2002**, *2*, 683–693.
- [7] K. Tanaka, Y. Fujii, H. Tokimoto, Y. Mori, S. Tanaka, G.-m. Bao, E. R. O. Siwu, A. Nakayabu, K. Fukase, *Chem. Asian J.* **2009**, *4*, 574–580, and references therein.
- [8] a) S. P. Vyas, A. Singh, V. Sihorkar, *Crit. Rev. Ther. Drug Carrier Syst.* **2001**, *18*, 1–76; b) M. Willis, E. Forssen, *Adv. Drug Delivery Rev.* **1998**, *29*, 249–271.
- [9] a) K. Tanaka, K. Minami, T. Tahara, Y. Fujii, E. R. O. Siwu, S. Nozaki, H. Onoe, S. Yokoi, K. Koyama, Y. Watanabe, K. Fukase, *ChemMedChem* **2010**, *5*, 841–845; b) K. Tanaka, K. Minami, T. Tahara, E. R. O. Siwu, K. Koyama, S. Nozaki, H. Onoe, Y. Watanabe, K. Fukase, *J. Carbohydr. Chem.* **2010**, *29*, 118–132; c) Lysine Labeling & Engineering Kit “STELLA+” from Kishida Chemical Co., Ltd., <http://www.kishida.co.jp/>.
- [10] K. Tanaka, T. Masuyama, K. Hasegawa, T. Tahara, H. Mizuma, Y. Wada, Y. Watanabe, K. Fukase, *Angew. Chem.* **2008**, *120*, 108–111; *Angew. Chem. Int. Ed.* **2008**, *47*, 102–105.
- [11] For representative examples of noninvasive imaging and biodistribution experiments, see: a) S. André, C. Unverzagt, S. Kojima, X. Dong, C. Fink, K. Kayser, H.-J. Gabius, *Bioconjugate Chem.* **1997**, *8*, 845–855; b) S. André, C. Unverzagt, S. Kojima, M. Frank, J. Seifert, C. Fink, K. Kayser, C.-W. von der Lieth, H.-J. Gabius, *Eur. J. Biochem.* **2004**, *271*, 118–134; c) S. André, S. Kojima, I. Prahl, M. Lensch, C. Unverzagt, H.-J. Gabius, *FEBS J.* **2005**, *272*, 1986–1998; d) S. André, S. Kojima, G. Gundel, R. Russwurm, X. Schratz, C. Unverzagt, H.-J. Gabius, *Biochim. Biophys. Acta Gen. Subj.* **2006**, *1760*, 768–782; e) S. André, T. Kozar, R. Schuberth, C. Unverzagt, S. Kojima, H.-J. Gabius, *Biochemistry* **2007**, *46*, 6984–6995; f) S. André, T. Kozar, S. Kojima, C. Unverzagt, H.-J. Gabius, *Biol. Chem.* **2009**, *390*, 557–565; g) M. V. Pimm, A. C. Perkins, J. Strohm, K. Ulbrich, R. Duncan, *J. Drug Targeting* **1996**, *3*, 385–390; h) M. I. M. Prata, A. C. Santos, S. Torres, J. P. André, J. A. Martins, M. Neves, M. L. Garcia-Martin, T. B. Rodrigues, P. Lopez-Larrubia, S. Cerdan, C. F. G. C. Geraldies, *Contrast Media Mol. Imaging* **2006**, *1*, 246–258; i) M. Hirai, H. Minematsu, N. Kondo, K. Oie, K. Igarashi, N. Yamazaki, *Biochem. Biophys. Res. Commun.* **2007**, *353*, 553–558; j) W. C. Chen, G. C. Completo, J. C. Paulson, *Glycobiology* **2008**, *18*, 963; k) S. T. Laughlin, J. M. Baskin, S. L. Amacher, C. R. Bertozzi, *Science* **2008**, *320*, 664–667; l) S. Serres, D. C. Anthony, Y. Jiang, K. A. Broom, S. J. Campbell, D. J. Tyler, S. I. van Kasteren, B. G. Davis, N. R. Sibson, *J. Neurosci.* **2009**, *29*, 4820–4828; m) S. I. van Kasteren, S. J. Campbell, S. Serres, D. C. Anthony, N. R. Sibson, B. G. Davis, *Proc. Natl. Acad. Sci. USA* **2009**, *106*, 18–23.
- [12] K. Tanaka, C. Kageyama, K. Fukase, *Tetrahedron Lett.* **2007**, *48*, 6475–6479.
- [13] Kind gifts from Otsuka Chemical Co., Ltd., <http://tansaku.otsukac.co.jp/en/oligo04.html>. These structurally pure N-glycans were isolated from egg yolk according to the procedure developed by Kajihara and co-workers: Y. Kajihara, Y. Suzuki, N. Yamamoto, K. Sasaki, T. Sakakibara, L. R. Juneja, *Chem. Eur. J.* **2004**, *10*, 971–985.
- [14] For representative reviews, see: a) R. Roy, M.-G. Beak, *Rev. Mol. Biotechnol.* **2002**, *90*, 291–309; b) M. A. Leeuwenburgh, G. A. van der Marel, H. S. Overkleeft, *Curr. Opin. Chem. Biol.* **2003**, *7*, 757–765; c) O. Renaudet, *Mini-Rev. Org. Chem.* **2008**, *5*, 274–286; d) Y. M. Chabre, R. Roy, *Curr. Top. Med. Chem.* **2008**, *8*, 1237–1285; e) Y. M. Chabre, R. Roy, *Advances in Carbohydrate Chemistry and Biochemistry, Vol. 63*, Elsevier, UK, **2010**, pp. 165–393.
- [15] As with previous reports on mass analysis of the sialosides, the molecular ions of the sialoglycocluster **3a** were observed as a more broadened peak consisting of partially desialylated derivatives (see the Supporting Information): Y. Fukuyama, S. Nakaya, Y. Yamazaki, K. Tanaka, *Anal. Chem.* **2008**, *80*, 2171–2179.
- [16] H. R. Maecke, M. Hofmann, U. Haberkorn, *J. Nucl. Med.* **2005**, *46*, 172S–178S.
- [17] A molecular diameter of 3 nm is known to smoothly clear through the kidney. Clusters **1** (molecular weight, MW = 10 000) and **3** (MW = 50 000) in the unfolded conformation are estimated roughly to be 3 and 7 nm in size, respectively: a) B. Haraldsson, J. Nyström, W. M. Deen, *Physiol. Rev.* **2008**, *88*, 451–487; b) A. Edwards, B. S. Daniels, W. M. Deen, *Am. J. Physiol. Renal Physiol.* **1999**, *276*, F892–F902.
- [18] A. R. Wyatt, J. J. Yerbury, S. Poon, M. R. Wilson, *Curr. Med. Chem.* **2009**, *16*, 2855–2866.
- [19] The opposite serum stability of neoglycoproteins in mice, that is, $\alpha(2-3)$ -sialylated derivatives show longer half-lives than the $\alpha(2-6)$ -sialylated congeners, has been reported when glycans were attached to albumin: C. Unverzagt, S. André, J. Seifert, S. Kojima, C. Fink, G. Srikrishna, H. Freeze, K. Kayser, H.-J. Gabius, *J. Med. Chem.* **2002**, *45*, 478–491.
- [20] R. Tozawa, S. Ishibashi, J. Osuga, K. Yamamoto, H. Yagyu, K. Ohashi, Y. Tamura, N. Yahagi, Y. Iizuka, H. Okazaki, K. Harada, T. Gotoda, H. Shimano, S. Kimura, R. Nagai, N. Yamada, *J. Biol. Chem.* **2001**, *276*, 12624–12628.
- [21] a) P. R. Crocker, A. Varki, *Immunology* **2001**, *103*, 137–145; b) P. R. Crocker, A. Varki, *Trends Immunol.* **2001**, *22*, 337–342; c) T. Angata, *Mol. Diversity* **2006**, *10*, 555–566; d) A. Varki, T. Angata, *Glycobiology* **2006**, *16*, 1R–27R.

- [22] E. I. Park, Y. Mi, C. Unverzagt, H.-J. Gabius, J. U. Baenziger, *Proc. Natl. Acad. Sci. USA* **2005**, *102*, 17125–17129.
- [23] Y. C. Lee, R. R. Townsend, M. R. Hardy, J. Lonngren, J. Arnarp, M. Haraldsson, H. Lonn, *J. Biol. Chem.* **1983**, *258*, 199–202.
- [24] a) T. Nakagawa, N. Uozumi, M. Nakano, Y. Mizuno-Horikawa, N. Okuyama, T. Taguchi, J. Gu, A. Kondo, N. Taniguchi, E. Miyoshi, *J. Biol. Chem.* **2006**, *281*, 29797–29806; b) E. Miyoshi, K. Noda, Y. Yamaguchi, S. Inoue, Y. Ikeda, W. Wang, J. H. Ko, N. Uozumi, W. Li, N. Taniguchi, *Biochim. Biophys. Acta Gen. Subj.* **1999**, *1473*, 9–20.
- [25] a) J. G. Cyster, C. C. Goodnow, *Immunity* **1997**, *6*, 509–517; b) B. E. Collins, O. Blixt, A. R. DeSieno, N. Bovin, J. D. Marth, J. C. Paulson, *Proc. Natl. Acad. Sci. USA* **2004**, *101*, 6104–6109; c) P. R. Crocker, J. C. Paulson, A. Varki, *Nat. Rev. Immunol.* **2007**, *7*, 255–266.
- [26] a) E. M. Comelli, S. R. Head, T. Gilmartin, T. Whisenant, S. M. Haslam, S. J. North, N. K. Wong, T. Kudo, H. Narimatsu, J. D. Esko, K. Drickamer, A. Dell, J. C. Paulson, *Glycobiology* **2006**, *16*, 117–131; b) H. Tateno, H. Y. Li, M. J. Schur, N. Bovin, P. R. Crocker, W. W. Wakarchuk, J. C. Paulson, *Mol. Cell. Biol.* **2007**, *27*, 5699–5710; c) M. K. O'Reilly, B. E. Collins, S. Han, L. Liao, C. Rillahan, P. I. Kitov, D. R. Bundle, J. C. Paulson, *J. Am. Chem. Soc.* **2008**, *130*, 7736–7745.
- [27] a) D. D. Manning, X. Hu, P. Beck, L. L. Kiessling, *J. Am. Chem. Soc.* **1997**, *119*, 3161–3162; b) J. D. Reuter, A. Myc, M. M. Hayes, Z. Gan, R. Roy, D. Qin, R. Yin, L. T. Piehler, R. Esfand, D. A. Tomalia, J. R. Baker, Jr., *Bioconjugate Chem.* **1999**, *10*, 271–278; c) S. André, H. Kaltner, T. Furuike, S.-I. Nishimura, H.-J. Gabius, *Bioconjugate Chem.* **2004**, *15*, 87–98; d) V. Ladmiral, G. Mantovani, G. J. Clarkson, S. Cauet, J. L. Irwin, D. M. Haddleton, *J. Am. Chem. Soc.* **2006**, *128*, 4823–4830; e) C. B. Carlson, P. Mowery, R. M. Owen, E. C. Dykhuizen, L. L. Kiessling, *ACS Chem. Biol.* **2007**, *2*, 119–127; f) M. L. Wolfenden, M. J. Cloninger, *Bioconjugate Chem.* **2006**, *17*, 958–966; g) J. Kim, Y. Ahn, K. M. Park, Y. Kim, Y. H. Ko, D. H. Oh, K. Kim, *Angew. Chem.* **2007**, *119*, 7537–7539; *Angew. Chem. Int. Ed.* **2007**, *46*, 7393–7395; h) M. J. Lee, K. Pal, T. Tasaki, S. Roy, Y. Jiang, J. Y. An, R. Banerjee, Y. T. Kwon, *Proc. Natl. Acad. Sci. USA* **2008**, *105*, 100–105.